THE ASTROPHYSICAL JOURNAL, 421:153–162, 1994 January 20

COMPTONIZATION OF DIFFUSE AMBIENT RADIATION BY A RELATIVISTIC JET: THE SOURCE OF GAMMA RAYS FROM BLAZARS?

MAREK SIKORA,[1,2] MITCHELL C. BEGELMAN,[1,3] AND MARTIN J. REES[4]

Received 1993 April 26; accepted 1993 July 30

ABSTRACT

Recent EGRET observations of blazars have revealed strong, variable gamma-ray fluxes with no signatures of gamma-ray absorption by pair production. This radiation probably originates from the inner parts of relativistic jets which are aimed nearly toward us. On sub-parsec scales, the jet will be pervaded by radiation from the broad-line region, as well as by photons from the central continuum source (some of which will be scattered by thermal plasma). In a frame moving with the relativistic outflow, the energy of this ambient radiation would be enhanced. This radiation would be Comptonized by both cold and relativistic electrons in the jet, yielding (in the observer's frame) a collimated beam of X-rays and gamma rays.

On the assumption that this process dominates self-Comptonization of synchrotron radiation, we develop a self-consistent model for variable gamma-ray emission, involving a single population of relativistic electrons accelerated by a disturbance in the jet. The spectral break between the X-ray and gamma-ray band, observed in 3C 279 and deduced for other blazars, results from inefficient radiative cooling of lower energy electrons. The existence of such a break strongly favors a model involving Comptonization of an external radiation field over a synchrotron self-Compton model. We derive constraints on such model parameters as the location and speed of the source, its dimensions and internal physical parameters, the maximum photon energies produced in the source, and the density and distribution of ambient radiation.

Finally, we discuss how observations might discriminate between our model and alternative ones invoking Comptonization of ambient radiation. Extension of gamma-ray spectra up to TeV energies (as observed in Mrk 421) is possible in an external Comptonization picture, provided that the ambient seed photons are in the infrared band (e.g., thermal emission by warm dust).

Subject headings: galaxies: jets — gamma rays: theory — radiation mechanisms: miscellaneous

1. INTRODUCTION

Recent observations by the EGRET instrument on *Compton Gamma Ray Observatory* show that many blazars (i.e., optically violently variable [OVV] quasars and BL Lac objects) are strong emitters of high-energy gamma rays. Their spectra above ~ 10 MeV typically have a power-law shape with a photon spectral index between 1.6 and 2.4, do not show any signatures of gamma-ray absorption by pair production up to energies as high as ~ 10 GeV, and show evidence of significant variability on timescales as short as days–weeks (Hartman et al. 1992; Hunter et al. 1993; Bertsch et al. 1993; Fichtel et al. 1993). These observations seem to support the theory that blazars are radio-loud active galactic nuclei (AGNs) with relativistic jets pointed toward us, and that their spectra are dominated by Doppler-boosted radiation of sub-parsec jets (Blandford & Rees 1978; Blandford & Königl 1979; Maraschi, Ghisellini, & Celotti 1992). Furthermore, the similarity between timescales of variability in gamma rays and other wavelength bands suggests that the gamma rays originate in the same parts of the jets as other strongly variable components.

Observationally, blazar spectra appear to be composed from at least two components: a low-energy component with luminosity (defined here as νF_ν, where F_ν is the spectral flux) peaking in the IR-UV range, and a high-energy component with luminosity strongly dominated by hard gamma rays, at least in those sources detected by EGRET. The division of spectra into two components is clearly reflected by the steep drop of the low-energy component toward the far-UV band (Impey & Neugebauer 1988; Brown et al. 1989a, b), and the rise of νF_ν toward higher energies in the X-ray band, observed clearly in most OVV quasars (Worrall & Wilkes 1990; Kii et al. 1992) and sometimes in BL Lac objects (Mushotzky et al. 1978). The X-ray spectra should "break" in slope at energies of a few MeV in order to join the gamma-ray spectra observed by EGRET, which have spectral indices $\alpha_\gamma > \alpha_X$. The break has been observed directly in 3C 279 and 3C 273 (Hermsen et al. 1993) and deduced for many other blazars from comparison of EGRET fluxes with the highest X-ray fluxes recorded in the past. We illustrate these features schematically in Figure 1.

The simplest models addressing the double-component nature of blazar spectra are those in which the low-energy component is produced by synchrotron radiation and the high-energy component is produced by the inverse-Compton process. The most widely studied models of this type are the so-called synchrotron self-Compton (SSC) models, originally suggested by Ginzburg & Syrovatski (1969) and developed in

[1] Joint Institute for Laboratory Astrophysics, University of Colorado and National Institute of Standards and Technology, Boulder, Colorado 80309; I: mitch@jila.colorado.edu.

[2] Copernicus Astronomical Center, Polish Academy of Sciences, Warsaw, Poland; I: sikora@camk.edu.pl.

[3] Also at Department of Astrophysical, Planetary, and Atmospheric Sciences, University of Colorado, Boulder.

[4] Institute of Astronomy, Cambridge, England, UK; I jm@ast-star.cam.ac.uk.

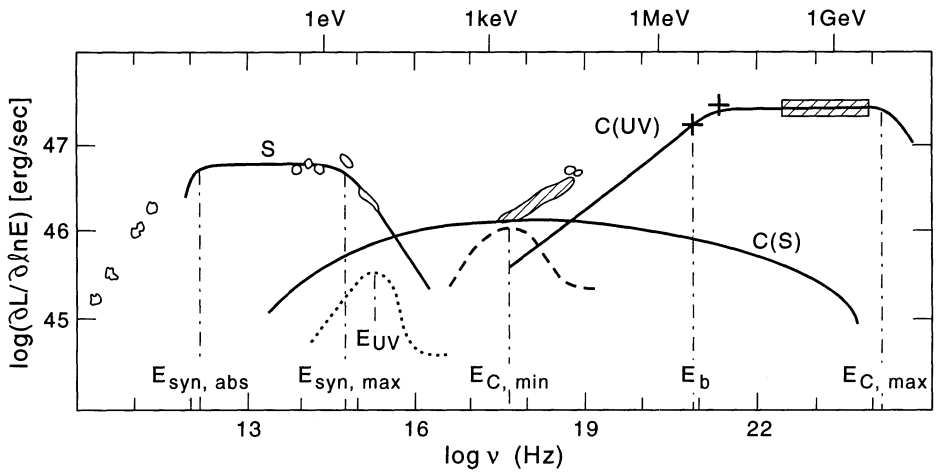

FIG. 1.—Spectrum of 3C 279. Solid lines mark the model spectrum components: (S): synchrotron radiation; C(S): Comptonized synchrotron radiation; and C(UV): Comptonized diffuse UV radiation. In addition, the central UV radiation spectrum is shown (*dotted line*), along with a possible component due to Comptonization of diffuse UV radiatiom by cold electrons in the jet (*dashed line*). Observations are depicted from the following sources: Makino et al. (1989) for the radio–X-ray range, during high states; Hermsen et al. (1993) for soft gamma-ray measurements from Comptel (*crosses*); and Hartman et al. (1992) for hard gamma-ray measurements from EGRET. The model parameters are specified in the text.

detail for spherical homogeneous sources by Rees (1967) and Jones, O'Dell, & Stein (1974). These models were later incorporated into the relativistic jet scenario (e.g., Königl 1981; Marscher & Gear 1985; Ghisellini & Maraschi 1989). SSC models have the elegant feature that the synchrotron photons are both produced and Comptonized by the same population of relativistic electrons. However, fitting an SSC model to observed blazar spectra is difficult (Bloom & Marscher 1993; Maraschi et al. 1992).

An alternative hypothesis is that the high-energy spectrum results not from the SSC mechanism, but from Comptonization of some source of radiation external to the jet. The most natural source of seed photons is the radiation from the central accretion flow, a portion of which is scattered or reprocessed by material in the region through which the jet is passing. Depending on the details of geometry and kinematics, the Compton interaction will be dominated by either the direct radiation field or the diffuse, reprocessed radiation field. Begelman & Sikora (1987) first pointed out that Compton scattering of ambient radiation by a cold relativistic jet could reproduce many of the distinctive features of blazar radiation, such as large, rapidly variable polarizations. The possibility of producing high-energy radiation by this kind of mechanism was studied by Melia & Königl (1989), who assumed enormous bulk Lorentz factors in the jet. However, similar effects could be achieved with more modest bulk Lorentz factors ($\sim O[10]$, similar to those inferred from radio observations of superluminal motion), provided that the radiating electrons have ultrarelativistic random energies in the fluid frame of the jet (e.g., Dermer, Schlickeiser, & Mastichiadis 1992).

In order for Compton scattering of external radiation to dominate over SSC emission, the energy density of the external radiation, as measured in the frame comoving with the jet, must exceed the energy density of synchrotron radiation produced in the jet. It is rather difficult to satisfy this condition by considering only direct radiation from the central source, as was originally proposed by Dermer et al. (1992). In order to avoid absorption of gamma rays by pair production on soft photons, the observed gamma rays must be produced in regions of the jet at distances $\geq 10^{17}$ cm, i.e., well outside the source of the radiation (see, e.g., Maraschi et al. 1992). At such distances the plasma in the jet, flowing at relativistic speeds, sees the radiation of the central source strongly redshifted. In order for this radiation to dominate over the local synchrotron radiation field, extremely weak magnetic fields are required.

To ameliorate this problem, Blandford (1993) and Sikora, Begelman, & Rees (1993) proposed that the dominant contribution to the energy density, as measured in the comoving frame of the radiating plasma, comes from scattered or reprocessed portions of the central source radiation, rather than from the direct radiation of the central source.[5] A diffuse radiation field, at large distances from the central source, can be produced by scattering off a hot accretion disk wind, by reprocessing in clouds producing broad emission lines, and by absorption and thermal reradiation of dust. Measured in the frame of a relativistic jet passing through the region of reprocessing, this radiation is strongly blueshifted. Sikora et al. (1993) showed that such a scenario can explain all basic features of the 3C 279 spectrum within a "one-zone" model, and the present paper presents the full version of this work. Specifically, we use the observed properties of the high-energy radiation to deduce the physical characteristics of the emitting region, and then show how the same region can produce lower energy synchrotron radiation having properties consistent with observations. This argument flows in the opposite direction to that normally used in SSC models, in which the high-energy radiation is deduced from low-frequency observations. We feel that this is more appropriate in the present case, since it is possible that regions larger than the one we consider contribute to (or even dominate) the low-frequency synchrotron emission.

We organize the paper as follows. In § 2 we discuss some general constraints which can be imposed on the kinematics

[5] Dermer (1993), Zbyszewska (1993), and Dermer & Schlickeiser (1993) attempt to address the same problem by proposing that the seed photons come from radii in the accretion disk which are comparable to the height of the jet-emitting region above the disk.

and geometry of a variable relativistic source by light-travel–time arguments. In §§ 3 and 4 we show how observable spectral features can be combined with variability arguments to derive the physical properties of the source. Finally, in § 5 we show how our model can quantitatively explain the multiwavelength observations of 3C 279 and discuss the possible application of the model to other EGRET sources, including the TeV gamma-ray source Mrk 421. Generic predictions of our model are discussed, along with comparisons between our model and those proposed by Blandford and by Dermer and collaborators. Although all three models invoke the Comptonization of external radiation impinging on the jet, there are important differences among them. In particular, our model is the only one of the three which seeks to synthesize both components of the blazar spectrum using a single population of relativistic electrons.

2. GEOMETRY AND KINEMATICS OF THE RADIATION SOURCE

We assume that blazar radiation is emitted by a relativistic jet which emanates from the central region of an AGN and propagates through the radiation field produced by matter accreting onto a supermassive black hole (see Fig. 2). The jet is composed of two plasma components, a cold one (i.e., with nonrelativistic random energies in the bulk fluid frame) and a relativistic one. Since relativistic particles are magnetically coupled to the cold plasma, we assume that the two components propagate along the jet with a single bulk Lorentz factor, $\Gamma \gg 1$ (speed $\beta \simeq 1$), and that the momentum distribution of relativistic particles is isotropic in the comoving frame. The velocity vector of the material emitting most of the observed radiation may lie anywhere within an angle $\theta_{\rm obs} \sim 1/\Gamma$ of the observer's line of sight, since the Doppler factor $\mathscr{D} \equiv \Gamma^{-1}(1 - \beta \cos \theta_{\rm obs})^{-1}$ has an approximately constant, maximum value of $\sim\Gamma$ over this range of angles, and declines rapidly outside this cone. Although an individual jet might be narrower than $\theta_{\rm obs}$, the orientations of typical blazar jets should be distributed uniformly within the cone bounded by $\theta_{\rm obs}$. It is quite plausible that individual jets are at least as broad as $\theta_{\rm obs}$, and that we observe a superposition of radiation emitted by jet material distributed throughout the cone. In either case, variability arguments relying on angular alignments more precise than $\sim 1/\Gamma$ (e.g., Marscher 1993) require special geometric arrangements beyond the selection effects produced by Doppler boosting; therefore they cannot be invoked to explain any phenomenon which is generic to blazars.

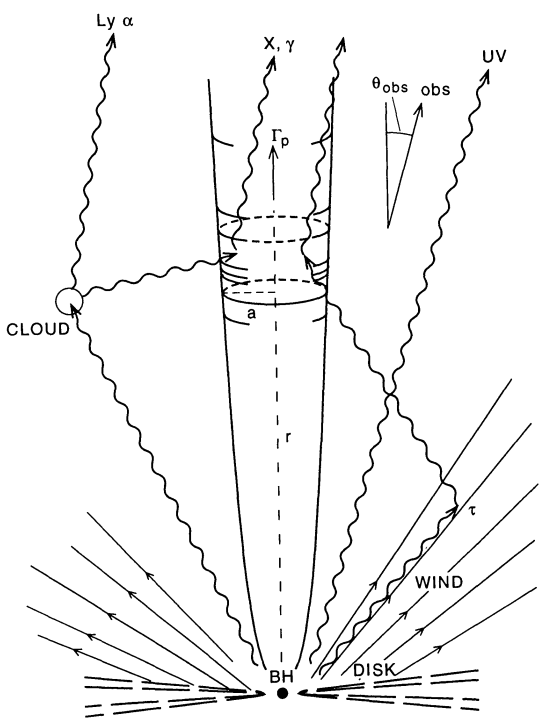

FIG. 2.—Geometry of the source. The radiating region, denoted by short cylinder of dimension a, moves along the jet with pattern Lorentz factor Γ_p. Underlying flow moves with Lorentz factor Γ, which may be different.

Blazar spectra during bright phases (hereafter called "flares") are assumed to be dominated by radiation from some time-dependent source pattern which propagates along the jet in a causal fashion. In this paper we construct a one-zone model, in the sense that both the IR-to-UV and X-ray-to-gamma-ray portions of the blazar spectrum are produced within the same region of the flow, by the same population of particles. This contrasts with Blandford's (1993) hypothesis that different spectral components are produced at different locations along the jet but does not preclude the possibility of additional spectral components. The extension of the gamma-ray spectrum up to GeV energies implies that the main emission region must lie at a distance $r \gg r_{\rm cen}$ from the central region of the accretion flow, where $r_{\rm cen}$ is the central source radius, in order to avoid absorption by photon-photon pair production on ambient radiation external to the jet. We further assume that the main contribution to the observed spectrum comes from a localized distance range $\Delta r \lesssim r$.

Since we do not know the nature of the disturbances leading to variability, we will characterize them generically using three parameters. We suppose that, in the frame comoving with the fluid, the *pattern* of the disturbance propagates down the jet with speed β'_p [Lorentz factor $\Gamma'_p \equiv (1 - \beta'^2_p)^{-1/2}$], causing a radiation "event" with a characteristic timescale $\Delta t'$. Here, as elsewhere in the paper, primed quantities denote measurements made in the comoving (fluid) frame, hence a disturbance with $\beta'_p = -\beta$ is stationary in the observer's frame. Each fluid element "triggered" by the disturbance is assumed to radiate for a time $\Delta t'_{\rm rad} \equiv \eta \Delta t'$, where $\eta \leq 1$.

Now let us relate these parameters to the observed characteristics of a flare. In the stationary "observer's" frame, a Lorentz transformation gives the total timescale of the "emission" as $(\Delta t)_{\rm em} \approx \Gamma \Delta t'(1 + \beta\beta'_p) + \Gamma \Delta t'_{\rm rad} = \Gamma \Delta t'(1 + \beta\beta'_p + \eta)$. Note that the appearance of the disturbance can be quite different in the two frames, particularly if the pattern is propagating upstream with $\beta'_p \approx -1$. In the comoving frame, a disturbance with $\eta \ll 1$ will appear as a short radiating zone moving along the jet. The duration of the flare in this frame therefore depends on the distance over which the radiating region propagates. In the observer's frame, however, a flare with $\eta > 1 + \beta\beta'_p$ will appear to turn on nearly all at once over its whole length, and the overall duration of the flare will be determined by the radiation timescale, not by the propagation timescale. Moreover, the variability timescale actually measured by the observer is compressed by light-travel–time effects, by a factor $(1 - \beta_p \cos \theta_{\rm obs})$ where $\beta_p = (\beta'_p + \beta)/(1 + \beta'_p\beta)$ is the pattern speed in the observer's frame. 3C 279 and many other blazars observed by EGRET exhibit superluminal motion of structure mapped with Very Long Baseline Interferometry (Fichtel et al. 1993), which requires relativistic pattern speeds for at least the radio-emitting

regions. We will therefore adopt the approximation $\Gamma_p \gg 1$ ($\beta_p \simeq 1$), although we will see later that relativistic pattern speeds are not needed to explain the observed high-energy gamma rays. If $\theta_{\rm obs} \approx 1/\Gamma$, the *observed* timescale of the flare is then given by

$$\Delta t \sim \frac{\Delta t'}{\Gamma}\frac{\eta + f_p}{f_p} \equiv \frac{\Delta t'}{\Gamma}\phi_p , \tag{1}$$

where

$$f_p \equiv \frac{\beta_p}{\Gamma^2(1-\beta_p\cos\theta_{\rm obs})} \approx 2\left(1+\frac{\Gamma^2}{\Gamma_p^2}\right)^{-1} \le 2 . \tag{2}$$

The parameter ϕ_p, which always exceeds one, represents the increase in apparent variability timescale (compared to the naive relativistic estimate) due to the propagation of the disturbance in the comoving frame. The distance traveled by the emitting region during the event, which places a lower limit on r, is given by

$$\Delta r \sim c\beta_p(\Delta t)_{\rm em} \equiv c\,\Delta t\Gamma^2 f_p . \tag{3}$$

Thus, f_p represents the effect of pattern propagation on the distance traveled by the disturbance, again compared to a simple relativistic estimate. In the comoving frame, the length of a region producing radiation at any one time is given by

$$a' \sim c\,\Delta t'_{\rm rad}|\beta'_p| \sim c\,\Delta t\Gamma\frac{\eta|\beta'_p|}{\phi_p} . \tag{4}$$

In our calculations below we will assume that all three source dimensions are of order a', and that the instantaneous radiation volume in the source frame is $V'_{\rm rad} \sim \pi a'^3$. Note that $\beta'_p \approx f_p - 1$, given our other approximations, and that $|\beta'_p|$ need not be close to one.

One must exercise care in using observed fluxes to derive energy densities in the comoving frame, for radiation produced within the flow. To calculate a naive "observed" luminosity L from an observed flux we multiply the latter by $4\pi d_L^2$, where d_L is the luminosity distance to the source. L is related to the emitted luminosity in the observer frame by $L \approx \Gamma^4 f_p L_{\rm em}$, where two powers of Γ come from the Doppler-beaming effect and the remaining factors account for light-travel–time compression. For frequency-integrated luminosities, or luminosities per logarithmic frequency interval, we have $L_{\rm em} = E_{\rm em}/(\Delta t)_{\rm em} \approx L'/(\eta + f_p)$, where $E_{\rm em}$ is the energy emitted during the flare and L' is the luminosity in the comoving frame. Relating L' to the radiation energy density through $L' \approx 4\pi c a'^2 u'_{\rm rad}$ we finally obtain the conversion between "observed" luminosity and the radiation energy density in the comoving frame,

$$u'_{\rm rad} \approx \frac{L}{4\pi c a'^2}\frac{\phi_p}{\Gamma^4} \approx \frac{L}{4\pi c^3(\Delta t)^2\Gamma^6}\frac{\phi_p^3}{\eta^2\beta_p'^2} . \tag{5}$$

3. ANALYSIS OF HIGH-ENERGY BLAZAR SPECTRA

In this section and the next, we deduce the properties of a source which could emit a gamma-ray flare like that observed in 3C 279, using observed variability timescales, luminosities, and spectral features as input. Our objective is to show how all of these properties follow from two simple and plausible assumptions: (1) that both the optical-UV and gamma-ray portions of the spectra are produced by the same population of electrons; and (2) that the spectral break between X-rays and gamma rays results from energy loss by the high-energy electrons.

3.1. *Comptonization of External Radiation versus Synchrotron Self-Compton Emission*

Comptonization of an external radiation field will dominate over synchrotron self-Compton emission if the energy density of the external radiation, as measured in the comoving frame, exceeds that of the internally produced synchrotron radiation. The best candidate for such external radiation is not direct radiation from the central source, which is strongly redshifted as measured in the source comoving frame, but a "diffuse" radiation field, i.e., a radiation field having a significant nonradial component at large distances from the central engine. Such a radiation component is inevitably produced in AGNs by scattering or reprocessing of a portion of the central radiation. Several mechanisms may contribute to the diffuse intensity, including line emission by irradiated clouds (dominated by Lyα), electron scattering in both clouds and intercloud medium (which preserves the shape of the incident UV continuum), and thermal infrared emission by irradiated dust.

In our calculations we adopt the approximation that the diffuse radiation field is isotropic as measured in a stationary frame coincident with the source. As viewed in the comoving frame, the angular dependence of frequency-integrated intensity varies with angle $\propto \mathscr{D}^4$, thus the approximation of isotropy is adequate provided that the intrinsic angular dependence is much weaker than this. In particular, all photons directed inward toward the central source are blueshifted by at least a factor Γ in the frame comoving with the jet. If these constitute of order half of the ambient photons, then the energy density of the diffuse radiation field, as measured in the comoving frame of the fluid, can be parametrized by

$$u'_{\rm diff} \simeq \Gamma^2 u_{\rm diff} \simeq \Gamma^2\tau L_{\rm UV}/4\pi r^2 c , \tag{6}$$

where $L_{\rm UV}$ is the luminosity of a central source (assumed here to be dominated by the UV bump) and τ is the fraction of the central luminosity forming the diffuse radiation field at distances $\sim r$. In the case of electron scattering τ will be roughly the Thomson optical depth across r; for reprocessing into lines it will be the fractional area covered by clouds times an efficiency factor.

As viewed from the comoving frame, about half of the ambient photons enter the jet from directions within an angle $\sim 1/\Gamma$ of the direction of motion. The mean energy of photons coming from all directions is $E'_{\rm ext} \sim \Gamma E_{\rm ext}$, where $E_{\rm ext}$ is the average energy of an ambient photon as measured in the local stationary frame. $E_{\rm ext}$ is a meaningful quantity where the diffuse radiation field has a relatively narrow energy distribution. In § 5.2 we show results for two such cases, one in which the diffuse radiation is dominated by UV energies ($E_{\rm ext} \sim 10$ eV) and the other in which near-infrared thermal radiation of dust dominates ($E_{\rm ext} \sim 0.4$ eV).

Photons scatttered by relativistic electrons (by which we mean either electrons or electron/positron pairs) in the source are isotropized in the comoving frame and their energies are boosted to $E' \sim \gamma^2 E'_{\rm ext}$, where γ is the electron random Lorentz factor as measured in the comoving frame. In the local stationary frame such photons are beamed along the velocity vector and those emitted into the direction $\theta_{\rm obs} \sim 1/\Gamma$ have energies

$$E \sim \Gamma E' \sim \Gamma^2\gamma^2 E_{\rm ext} . \tag{7}$$

The hard gamma rays from blazars measured with EGRET characteristically have power-law spectra with spectral indices $\alpha_\gamma \equiv -\partial \ln L_\gamma/\partial \ln E$ in the range 0.6–1.6 (Fichtel et al. 1993). The hard gamma-ray spectral index of the best-studied case

3C 279 is close to one, and we will adopt $\alpha_\gamma = 1$ as the fiducial case for computational simplicity. At observed energies below $E_b \lesssim 10$ MeV, the spectrum of 3C 279 and other blazars must break to lower values of the spectral index, in order to connect smoothly with observed X-ray fluxes. Such a spectral break is presumably due either to the superposition of spectra from an inhomogeneous source (Maraschi et al. 1992) or, especially in the case of a one-zone model, to a break in the electron energy distribution. While the latter could be the result of the particle injection process, we adopt the more economical hypothesis that E_b corresppnds to the electron Lorentz factor, γ_b, at which the timescale of radiative cooling is equal to the advection timescale through the radiating region. As is well known, the observed Compton and synchrotron spectra produced by a steadily injected power-law distribution of electrons steepens by $\Delta\alpha = 0.5$ above E_b (see § 4.1). A break of this magnitude agrees roughly with existing observations. We therefore adopt the X-ray spectral index $\alpha_X = 0.5$ in our calculations.

In order for relativistic Comptonization to yield a well-defined spectral break due to cooling there must be a simple mapping between γ_b and E_b. Such a mapping will exist only if the "seed" photons for Comptonization have a relatively narrow spectral peak. This is not the case if the seed photons come from internally produced synchrotron radiation, since the latter has too broad a spectrum (Fig. 1). However, if the diffuse radiation field comprises scattered UV bump radiation, UV line emission, or thermal radiation from dust with a narrow range of temperatures, then

$$\gamma_b \sim \frac{1}{\Gamma}\left(\frac{E_b}{E_{\rm ext}}\right)^{1/2} . \tag{8}$$

The Compton cooling condition is then given by $\gamma/\dot{\gamma} \sim m_e c/\gamma_b \sigma_T u'_{\rm rad} \sim \Delta t'_{\rm rad}$. Combining this condition with equations (1) and (8), we obtain

$$u'_{\rm rad} \sim \frac{m_e c}{\sigma_T \Delta t}\left(\frac{E_{\rm ext}}{E_b}\right)^{1/2}\frac{\phi_p}{\eta} . \tag{9}$$

Substituting $u'_{\rm diff}$ for $u'_{\rm rad}$ (eq. [6]) with $r \gtrsim \Delta r$ (eq. [3]) then gives

$$\tau L_{\rm UV} \sim \frac{4\pi m_e c^4 \Delta t \Gamma^2}{\sigma_T}\left(\frac{E_{\rm ext}}{E_b}\right)^{1/2}\left(\frac{r}{\Delta r}\right)^2\frac{\phi_p f_p^2}{\eta} . \tag{10}$$

For 3C 279 (Fig. 1), if we take $E_{\rm ext}/E_b \sim 10^{-6}$ and $\Delta t \sim 2$ days, then $u'_{\rm rad} \sim 0.24\phi_p/\eta$ ergs cm^{-3} and $\tau L_{\rm UV} \gtrsim 2.4 \times 10^{42}\Gamma^2\phi_p f_p^2/\eta$ ergs s^{-1}.

The ratio of SSC losses to losses due to Compton scattering on the external radiation field is given by $u'_{\rm syn}/u'_{\rm diff}$, where $u'_{\rm syn}$, the comoving synchrotron energy density, is estimated by substituting the "observed" luminosity of the synchrotron component $L_{\rm syn}$ into equation (5). Suppose we are able to place an observational upper bound on this ratio, say, $u'_{\rm syn}/u'_{\rm diff} < \zeta < 1$; then

$$\Gamma \gtrsim \left[\frac{\sigma_T}{4\pi m_e c^4}\frac{L_{\rm syn}}{\zeta\,\Delta t}\left(\frac{E_b}{E_{\rm ext}}\right)^{1/2}\frac{\phi_p^2}{\eta\beta_p'^2}\right]^{1/6} . \tag{11}$$

Plugging in the numbers quoted above for 3C 279, we obtain $\Gamma \gtrsim 5.9(L_{\rm syn,\,47}\,\phi_p^2/\zeta\eta\beta_p'^2)^{1/6}$, where $L_{\rm syn,\,47} \equiv L_{\rm syn}/10^{47}$ ergs s^{-1}. Note how insensitive this estimate is to the many uncertainties which have gone into the calculation.

Observationally, ζ is constrained to be substantially less than one in 3C 279 by the relatively low power output in the EUV–soft X-ray band (Fig. 1). A large fraction of the SSC radiation would lie in this band, whereas the radiation resulting from scattering of ambient UV yields a much harder X-ray spectrum and indeed contributes very little at energies below $\Gamma^2 E_{\rm ext}$, i.e., at energies ~ 1 keV for Comptonization of diffuse UV radiation with $\Gamma \sim 10$. Observations of blazars also indicate that the component which we identify with beamed synchrotron emission falls off in the UV. Therefore, there is a "gap" between the two main radiation components, primarily in the EUV–soft X-ray band, which could be partially filled in by SSC radiation. Soft X-ray flux measurements could place useful limits on ζ, e.g., $\zeta < (\partial L_{\rm SX}/\partial \ln E)/(\partial L_\gamma/\partial \ln E)$, where $(\partial L_{\rm SX}/\partial \ln E)$ and $(\partial L_\gamma/\partial \ln E)$ are the observed soft X-ray and gamma-ray luminosities per logarithmic energy bin.

3.2. *Maximum Energy of Comptonized External Photons*

Our assumption that both the synchrotron and Compton-scattered components of the spectrum are produced in the same region and by the same population of ultrarelativistic electrons corresponds to the relation $L_C/L_{\rm syn} = u'_{\rm diff}/u'_B$, where L_C is the inferred luminosity in the Compton component and u'_B is the energy density of the magnetic field in the comoving frame. Hence, the magnetic field intensity is given by $B' = [8\pi(L_{\rm syn}/L_C)u'_{\rm diff}]^{1/2}$ where $L_{\rm syn}/L_C \simeq (\partial L_{\rm syn}/\partial \ln E)/(\partial L_\gamma/\partial \ln E)$ is an observable quantity. Using equation (9), we obtain

$$B' = \left[\frac{8\pi m_e c}{\sigma_T \Delta t}\frac{\partial L_{\rm syn}/\partial \ln E}{\partial L_\gamma/\partial \ln E}\left(\frac{E_{\rm ext}}{E_b}\right)^{1/2}\frac{\phi_p}{\eta}\right]^{1/2} {\rm G} . \tag{12}$$

Taking the ratio of synchrotron to gamma-ray components in 3C 279 to be ~ 0.2 and setting other quantities as before, we obtain $B' \sim 1.1(\phi_p/\eta)^{1/2}$ G.

Now, using a δ-function approximation to relate the energy of a synchrotron photon to the electron Lorentz factor, we can estimate the maximum electron energy from the turnover frequency of the observed synchrotron spectrum, $E_{\rm syn,\,max} \simeq \Gamma E'_{\rm syn,\,max} \simeq \Gamma\gamma_{\rm max}^2(B'/B_{\rm cr})m_e c^2$, where $B_{\rm cr} = 2\pi m_e^2 c^3/he \approx 4.4 \times 10^{13}$ G. Thus, the maximum electron Lorentz factor is

$$\gamma_{\rm max} \simeq \left(\frac{B_{\rm cr}}{\Gamma B'}\frac{E_{\rm syn,\,max}}{m_e c^2}\right)^{1/2} \tag{13}$$

and the upper limit of the Compton spectrum, $E_{C,\,\rm max} \simeq \Gamma E'_{C,\,\rm max} \simeq \Gamma\gamma_{\rm max}^2 E'_{\rm ext} \simeq \gamma_{\rm max}^2\Gamma^2 E_{\rm ext}$, is given by

$$E_{C,\,\rm max} \simeq \frac{B_{\rm cr}}{B'}\frac{E_{\rm syn,\,max}}{m_e c^2}\Gamma E_{\rm ext} , \tag{14}$$

where B' is given by equation (12). Thus, taking $E_{\rm syn,\,max} \sim 5$ eV for 3C 279, we predict that the spectral component due to Comptonized external radiation should turn over at roughly $\sim 39(\Gamma/10)(E_{\rm ext}/10\ {\rm eV})$ GeV. This is not far above the current limits of EGRET observations of the high state.

3.3. *Constraints from Pair Production Opacity*

Even if photons with energies as high as $E_{C,\,\rm max}$ are produced in blazar jets, they could be prevented from escaping by pair production against soft photons. The lack of any pair absorption signatures in blazar spectra implies that the optical depth for pair production, $\tau_{\gamma\gamma}$, must be smaller than one. We will consider separately pair production on the external diffuse radiation field and on X-rays produced internally in the jet. Gamma rays can also be absorbed by photons coming directly from the central source. However, since $r/r_{\rm cen} \gg \Gamma$, such interactions are very inefficient because they can take place only at

angles $\sim 1/\Gamma$, at which their rate is reduced by a factor $\sim\Gamma^{2+\alpha}$ compared to an isotropic distribution of radiation with the same energy density and spectral index α.

The optical thickness for absorption of GeV photons in the external diffuse radiation field can be found from

$$\tau_{\gamma\gamma}^{(\mathrm{diff})}(E_\gamma) \sim \frac{\tau_{\mathrm{XUV}}(\partial L_{\mathrm{XUV}}/\partial \ln E)\sigma_{\gamma\gamma} E_\gamma}{4\pi c (m_e c^2)^2 r}, \quad (15)$$

where $\partial L_{\mathrm{XUV}}/\partial \ln E$ is the luminosity at $E \sim (m_e c^2)^2/E_\gamma$ and τ_{XUV} is the fraction of that luminosity present in a diffuse component at r. Note that τ_{XUV} can be much smaller than τ, if the production of a diffuse radiation field is dominated by processes other than Thomson scattering. Defining $(\tau_{\mathrm{XUV}}\partial L_{\mathrm{XUV}}/\partial \ln E)/(\tau L_{\mathrm{UV}}) \equiv f_{\mathrm{XUV}}^{(\mathrm{diff})}$ and using equations (3) and (10), we obtain

$$\tau_{\gamma\gamma}^{(\mathrm{diff})}(E_\gamma) \sim \frac{\sigma_{\gamma\gamma}}{\sigma_T} f_{\mathrm{XUV}}^{(\mathrm{diff})} \frac{E_\gamma}{m_e c^2}\left(\frac{E_{\mathrm{ext}}}{E_b}\right)^{1/2}\left(\frac{r}{\Delta r}\right)\frac{\phi_p f_p}{\eta}. \quad (16)$$

Since the spectrum of diffuse radiation peaks at energies well below the XUV energies needed for pair production, we can assume $f_{\mathrm{XUV}}^{(\mathrm{diff})} \ll 1$. Substituting the maximum value of the pair production cross section $\sim\sigma_T/5$, we find that gamma rays can escape through the diffuse radiation field up to an energy in excess of $2(\Delta r/r)(\eta/f_{\mathrm{XUV}}^{(\mathrm{diff})}\phi_p f_p)$ GeV, for $E_b/E_{\mathrm{ext}} \gtrsim 10^6$ (as in 3C 279).

For internally produced X-rays with a power-law spectral index α_X,

$$\tau_{\gamma\gamma}^{(\mathrm{int})}(E'_\gamma) \sim \frac{\sigma_{\gamma\gamma}[\partial L_X'^{(\mathrm{int})}/\partial \ln E']}{4\pi c a' E'_X}. \quad (17)$$

Taking into account that $\partial L_X'^{(\mathrm{int})}/\partial \ln E' \simeq (\partial L'_\gamma/\partial \ln E')(E'_X/E'_b)^{1-\alpha_X}$, $E'_X \simeq (m_e c^2)^2/E'_\gamma \simeq \Gamma(m_e c^2)^2/E_\gamma$, and $\partial L'_\gamma/\partial \ln E' \simeq (\partial L_\gamma/\partial \ln E)\phi_p/\Gamma^4$; and setting $\alpha_X \simeq 0.5$, we obtain

$$\tau_{\gamma\gamma}^{(\mathrm{int})}(E_\gamma) \sim \frac{\sigma_{\gamma\gamma}(\partial L_\gamma/\partial \ln E)}{4\pi m_e c^4 \Delta t \Gamma^5}\left(\frac{E_\gamma}{E_b}\right)^{1/2}\frac{\phi_p^2}{\eta|\beta'_p|}. \quad (18)$$

Equation (18) can be used to establish the necessity of relativistic beaming in a one-zone model for 3C 279, since $\tau_{\gamma\gamma}^{(\mathrm{int})}(E_\gamma) < 1$ implies that $\Gamma > 2.4(\partial L_\gamma/\partial \ln E)_{47}^{1/5}(E_\gamma/1\ \mathrm{GeV})^{1/10}(\Delta t/2\ \mathrm{d})^{-1/5}$. In fact, for our "best guess" models of 3C 279 (Table 1), the pair production constraint due to internally produced radiation is much weaker than that due to the external diffuse radiation field.

3.4. *Comptonization by Cold Electrons in Jet*

In addition to relativistic electrons, the jet may also contain "cold" plasma, i.e., particles with nonrelativistic energies in the comoving frame. Cold electrons will also Comptonize the diffuse external radiation, yielding a spectral component peaked around energies $E_{C,\mathrm{min}} \sim \Gamma^2 E_{\mathrm{ext}}$. (We denote this energy $E_{C,\mathrm{min}}$ because it corresponds to the lower end of the relativistic Comptonized component if the electron energy distribution extends down to random Lorentz factors $\gamma_{\mathrm{min}} \sim 1$.) One can place an upper limit on the amount of such cold plasma by measuring the radiation flux at $E_{C,\mathrm{min}}$.

From timescale arguments, the maximum dimension of the jet that can contribute to the variable emission is $a'_{\mathrm{max}} \sim c\Delta t\Gamma|\beta'_p|/\phi_p$. Suppose the Thomson optical depth across this region due to cold electrons is τ_j. Of the power τL_{UV} available in diffuse radiation, a fraction $\sim(a'_{\mathrm{max}}/r)^2\tau_j$ is scattered by the cold plasma into the direction $\theta_{\mathrm{obs}} \sim 1/\Gamma$. The observer therefore concludes that the scattered power is

$$L_{C,\mathrm{cold}} \sim \tau_j \tau L_{\mathrm{UV}}\left(\frac{a'_{\mathrm{max}}}{r}\right)^2\Gamma^6 \sim \tau_j \frac{4\pi m_e c^4 \Delta t \Gamma^6}{\sigma_T}\left(\frac{E_{\mathrm{ext}}}{E_b}\right)^{1/2}\frac{\beta_p'^2}{\eta\phi_p}, \quad (19)$$

TABLE 1

OUTPUT PARAMETERS FOR 3C 279, FOR INPUT PARAMETERS GIVEN IN TEXT

Quantity	Numerical Value	Parameter Dependence and Units
E_{ext}	(10, 0.4)	eV
Γ_{min}	(11.3, 14.8)	$\eta^{-1/6}\lvert\beta'_p\rvert^{-1/3}\phi_p^{1/3}$
Δr	$(6.6, 11) \times 10^{17}$	$(\Gamma/\Gamma_{\mathrm{min}})^2\eta^{-1/3}\lvert\beta'_p\rvert^{-2/3}\phi_p^{2/3}f_p$ cm
a'	$(5.9, 7.7) \times 10^{16}$	$(\Gamma/\Gamma_{\mathrm{min}})\eta^{5/6}\lvert\beta'_p\rvert^{2/3}\phi_p^{-2/3}$ cm
γ_b	(89, 340)	$(\Gamma/\Gamma_{\mathrm{min}})^{-1}\eta^{1/6}\lvert\beta'_p\rvert^{1/3}\phi_p^{-1/3}$
γ_{max}	$(5.6, 7.4) \times 10^3$	$(\Gamma/\Gamma_{\mathrm{min}})^{-1/2}\eta^{1/3}\lvert\beta'_p\rvert^{1/6}\phi_p^{-5/12}$
B'	(1.2, 0.53)	$\eta^{-1/2}\phi_p^{1/2}$ G
$E_{C,\mathrm{max}}$	(41, 4.7)	$(\Gamma/\Gamma_{\mathrm{min}})\eta^{1/3}\lvert\beta'_p\rvert^{-1/3}\phi_p^{-1/6}$ GeV
$E_{C,\mathrm{min}}$	(1.3, 0.087)	$(\Gamma/\Gamma_{\mathrm{min}})^2\eta^{-1/3}\lvert\beta'_p\rvert^{-2/3}\phi_p^{2/3}$ keV
$\nu_{\mathrm{syn,abs}}$	$(9.2, 6.8) \times 10^{11}$	$(\Gamma/\Gamma_{\mathrm{min}})^{-5/7}\eta^{-11/21}\lvert\beta'_p\rvert^{-1/3}\phi_p^{29/42}$ Hz
$\nu_{\mathrm{syn},b}$	$(2.9, 25) \times 10^{11}$	$(\Gamma/\Gamma_{\mathrm{min}})^{-1}\eta^{-1/3}\lvert\beta'_p\rvert^{1/3}\phi_p^{1/6}$ Hz
u'_{diff}	$(24, 4.7) \times 10^{-2}$	$\eta^{-1}\phi_p$ ergs cm^{-3}
u'_B	$(5.7, 1.1) \times 10^{-2}$	$\eta^{-1}\phi_p$ ergs cm^{-3}
u'_e	(0.62, 0.15)	$(\Gamma/\Gamma_{\mathrm{min}})^{-6}\eta^{-1}\lvert\beta'_p\rvert^{-1}\phi_p$ ergs cm^{-3}
Γ_{eq}	(16.9, 22.9)	$\eta^{-1/6}\lvert\beta'_p\rvert^{-1/2}\phi_p^{1/3}$
$\tau_{\gamma\gamma}^{(\mathrm{diff})}(10\ \mathrm{GeV})$	(3.9, 0.78)	$f_{\mathrm{XUV}}^{(\mathrm{diff})}\eta^{-1}\phi_p f_p$
$\tau_{\gamma\gamma}^{(\mathrm{diff})}(E_{C,\mathrm{max}})$	(16, 0.37)	$(\Gamma/\Gamma_{\mathrm{min}})f_{\mathrm{XUV}}^{(\mathrm{diff})}\eta^{-2/3}\lvert\beta'_p\rvert^{-1/3}\phi_p^{5/6}f_p$
$\tau_{\gamma\gamma}^{(\mathrm{int})}(10\ \mathrm{GeV})$	$(4.3, 1.1) \times 10^{-3}$	$(\Gamma/\Gamma_{\mathrm{min}})^{-5}\eta^{-1/6}\lvert\beta'_p\rvert^{2/3}\phi_p^{1/3}$
$\tau_{\gamma\gamma}^{(\mathrm{int})}(E_{C,\mathrm{max}})$	$(8.7, 0.77) \times 10^{-3}$	$(\Gamma/\Gamma_{\mathrm{min}})^{-9/2}\lvert\beta'_p\rvert^{1/2}\phi_p^{1/4}$
τL_{UV}	$(3.1, 1.1) \times 10^{44}$	$(\Gamma/\Gamma_{\mathrm{min}})^2\eta^{-4/3}\lvert\beta'_p\rvert^{-2/3}\phi_p^{5/3}f_p^2$ ergs s^{-1}
$\tau_{j,\mathrm{max}}$	$(2.0, 2.0) \times 10^{-3}$	$(\Gamma/\Gamma_{\mathrm{min}})^{-6}\eta^2\phi_p^{-1}$

where we have used equation (10) for $\tau L_{\rm UV}$. Note the strong dependence on Γ. Two powers of this come from the relativistic beaming, two come from the average photon energy amplification, and the remaining two are associated with light-travel–time compression. Apparently, a large value of Γ implies strong constraints on the amount of cold plasma carried by the jet.

3.5. *Synchrotron Self-Absorption*

The frequency below which synchrotron self-absorption cuts off the spectrum can be estimated from the observed properties of the radiation at higher energies. For a power-law electron distribution with energy index $p = 3$ we find that $\tau_{\rm syn,abs} \sim 1$ for

$$\nu_{\rm syn,abs} \sim 2 \times 10^8 \left(\frac{B'}{\Gamma}\right)^{1/7} \left[\frac{(\partial L_{\rm syn}/\partial \ln E)\phi_p}{a'^2}\right]^{2/7} \text{Hz}\,, \quad (20)$$

where all dimensional quantities are in cgs units. Taking $\partial L_{\rm syn}/\partial \ln E \sim 7 \times 10^{46}$ ergs s^{-1} and adopting other parameters quoted earlier for 3C 279, we estimate $\nu_{\rm syn,abs} \sim 4 \times 10^{12} \Gamma^{-5/7} \phi_p^{13/14} \eta^{-9/14} |\beta'_p|^{-4/7}$ Hz for this source, during a flaring episode. Since $\nu_{\rm syn,abs}$ is of the same order as $\nu_{{\rm syn},b}$, the characteristic synchrotron frequency emitted by electrons with Lorentz factors $\sim \gamma_b$ (see Table 1), we make little error by using the slope of the cooled electron distribution in estimating $\nu_{\rm syn,abs}$.

4. ENERGY AND MOMENTUM BUDGET

4.1. *Electron Energy Distribution*

During a flare, relativistic electrons are injected into the emission region according to the power-law function $Q = C_Q \gamma^{-q}$, where Q is the number of electrons injected per unit time and energy, integrated over the whole emitting volume. For the fiducial model with $\alpha_\gamma \simeq 1$ (appropriate for 3C 279), $q \simeq 2$, corresponding to an equal power injected per logarithmic energy band:

$$\frac{\partial P'_{\rm inj}}{\partial \ln \gamma} \simeq C_Q m_e c^2\,. \quad (21)$$

According to our interpretation of the spectral break at E_b, electrons suffer strong inverse Compton losses at $\gamma > \gamma_b$, and evolve adiabatically at $\gamma < \gamma_b$. Given the radiation time scale $\Delta t'_{\rm rad}$, the electron energy distribution is readily derived from a kinetic equation:

$$\frac{\partial N'_e}{\partial \ln \gamma} \simeq C_Q \Delta t'_{\rm rad} \times \begin{cases} 1/\gamma & \text{for } \gamma < \gamma_b \\ \gamma_b/\gamma^2 & \text{for } \gamma \geq \gamma_b \end{cases}\,. \quad (22)$$

Note that the slope of the electron energy distribution changes from $p = 3$ at $\gamma > \gamma_b$ to $p = 2$ at $\gamma < \gamma_b$. It is this effect that gives rise to the change of radiation spectral index from $\alpha_\gamma \simeq 1$ at $E > E_b$ to $\alpha_X \simeq 0.5$ at $E < E_b$.

C_Q can be related to the observed gamma-ray luminosity as follows. Since all electrons with $\gamma > \gamma_b$ are cooled effectively and the cooling is dominated by the Compton process with most energy released in gamma rays, the injected power per logarithmic energy band, $\partial P'_{\rm inj}/\partial \ln \gamma$, is approximately equal to $2\partial L'_\gamma/\partial \ln E' \simeq 2(\partial L_\gamma/\partial \ln E)\phi_p/\Gamma^4$ (where the factor 2 comes from $E'_C \propto \gamma^2$ for Compton scattering). Substituting this into equation (21), we find

$$C_Q = \frac{2(\partial L_\gamma/\partial \ln E)\phi_p}{\Gamma^4 m_e c^2}\,. \quad (23)$$

4.2. *Plasma Energy versus Magnetic Energy*

The ratio of plasma energy density to magnetic energy density is an important parameter from the point of view of acceleration processes and source confinement. Provided there is no relativistic hadronic component or significant thermal plasma, the plasma energy density is given by $u'_e = (m_e c^2/V'_{\rm rad}) \int_1^{\gamma_{\max}} (\partial N'_e/\partial \ln \gamma) d\gamma$, where $V'_{\rm rad} \approx \pi a'^3$ is the proper volume of the radiating region. Using equations (22) and (23), we obtain

$$u'_e = m_e c^2 \Delta t'_{\rm rad} C_Q \frac{(1 + \ln \gamma_b)}{V'_{\rm rad}} \sim \frac{2(\partial L_\gamma/\partial \ln E)\bar{\gamma}}{\pi c^3 (\Delta t)^2 \Gamma^6} \frac{\phi_p^3}{|\beta'_p|^3 \eta^2}\,, \quad (24)$$

where $\bar{\gamma} = \int (\partial N'_e/\partial \ln \gamma) d\gamma / \int (\partial N'_e/\partial \ln \gamma) \gamma^{-1} d\gamma = 1 + \ln \gamma_b$ is the average electron energy. Now, taking into account that $u'_B = u'_{\rm diff}(\partial L_{\rm syn}/\partial \ln E)/(\partial L_\gamma/\partial \ln E)$, we find that the ratio of plasma energy to magnetic energy is

$$\frac{u'_e}{u'_B} \sim \frac{2\sigma_T \bar{\gamma}}{\pi m_e c^4 \Delta t \Gamma^6} \left(\frac{E_b}{E_{\rm ext}}\right)^{1/2} \frac{(\partial L_\gamma/\partial \ln E)^2}{(\partial L_{\rm syn}/\partial \ln E)} \frac{\phi_p^2}{\eta |\beta'_p|^3}\,. \quad (25)$$

For the adopted 3C 279 parameters (§ 5.2) and noting that the rightmost factor accounting for pattern propagation effects always exceeds one, equation (25) gives $u'_e/u'_B \gtrsim 8 \times 10^6/\Gamma^6$. This implies that highly relativistic ($\Gamma \gtrsim 10$) speeds are required if the particle pressure is not greatly to exceed the magnetic pressure.

5. RESULTS AND DISCUSSION

5.1. *General Predictions and Comparison with Related Models*

Our model for high-energy blazar emission shares a fundamental assumption with the models proposed by Blandford (1993), by Dermer and collaborators (Dermer et al. 1992; Dermer 1993; Dermer & Schlickeiser 1993), and by Zbyszewska (1993), namely, that the high-energy emission from blazars results from the Comptonization of ambient radiation (i.e., radiation originating *outside* the jet) by relativistic electrons in a relativistic jet.

Like Blandford, we argue that the most plausible origin for the ambient radiation field is the scattering and/or reprocessing of radiation from the central source by material external to the jet, whereas Dermer et al. propose that the seed photons come from the accretion disk. Like Dermer et al., we propose that the steepening of the spectrum between the X-ray and gamma-ray bands results from cooling of the high-energy portion of the relativistic electron distribution, whereas Blandford derives this feature, and the shape of the gamma-ray spectrum, from the superposition of spectra produced over a large range of radii along the jet. Thus, a key prediction of our model, and of Dermer's, is that the change in slope across the break should always be observed to be ≈ 0.5; in Blandford's scenario, the change in slope is not determined. Moreover, Blandford proposes that gamma-rays of a given energy come mainly from the smallest radius from which they can escape without producing pairs, whereas we (and Dermer) assume that the observed gamma-ray spectrum is all produced at roughly the same radius from the central source. Thus, we would expect fluctuations in the gamma-ray flux to occur more or less coherently across a wide range of energies (although the energy of the spectral break may vary: see § 5.4), whereas Blandford predicts that the variability timescale should increase with increasing gamma-ray photon energy.

Our model is more tightly constrained than either of the alternative models, since we have attempted to explain both

the low- and high-energy components of the blazar spectrum using the same population of relativistic electrons. Thus, we additionally predict that the slope of the optical-UV blazar spectrum should be similar to that of the hard gamma rays, and that the two components should vary in phase. These predictions may be weakened somewhat if additional radiation components are present (e.g., in OVV quasars where a UV bump is present) or if the magnetic field strength is highly inhomogeneous across the region through which the disturbance is propagating.

5.2. *Results for 3C 279*

Table 1 lists numerical values for the parameters discussed in §§ 2–4, as functions of Γ and Γ_p for the two cases $E_{\rm ext} = 10$ eV and 0.4 eV. The following assumed input parameters are based on observations of 3C 279 presented in Hartman et al. (1992): $\Delta t \sim 2$ days; $\partial L_\gamma/\partial \ln E \sim 3 \times 10^{47}$ ergs s^{-1}; $\partial L_{\rm syn}/\partial \ln E \sim 7 \times 10^{46}$ ergs s^{-1}; $L_{\rm syn} \sim 5 \times 10^{47}$ ergs s^{-1}; $E_{\rm syn,max} \sim 5$ eV; $E_b \sim 10$ MeV; and $E_{\rm max} \gtrsim 10$ GeV. We normalize Γ to a minimum value, $\Gamma_{\rm min}$, given by equation (11) with $\zeta = 0.1$. The adopted value of ζ, and other relative normalizations of X- and gamma-ray fluxes, were chosen under the assumption that the soft X-ray luminosity during the gamma-ray flare observed by EGRET was of the same order as the luminosity of the brightest X-ray flare detected in the past. Since there were no X-ray observations of 3C 279 simultaneous with the gamma-ray flare reported by Hartman et al. (1992), the numbers in Table 1 should be regarded as illustrative only. Values for $\tau_{\gamma\gamma}^{\rm (diff)}$ and $\tau L_{\rm UV}$ were calculated assuming that $\Delta r \sim r$, so they should be regarded as lower limits. The upper limit on the Thomson optical depth of the cold plasma component in the jet, $\tau_{j,\rm max}$ (see eq. [19]) is computed under the assumption that $L_{C,\rm cold} \lesssim 10^{46}$ ergs s^{-1}.

Given our assumption that the spectral break at E_b results from cooling of the most energetic electrons on a flow timescale, $\Gamma_{\rm min}$ has the following physical significance. If Γ exceeds $\Gamma_{\rm min}$, then the SSC mechanism, acting on the observed synchrotron component, cannot account for the observed high-energy portion of the spectrum. Production of the gamma-ray spectrum by Compton scattering then requires an alternative source of seed photons, which we conjecture to be a diffuse radiation field surrounding the jet. The plausibility of this hypothesis is shown by our estimate of $\Gamma_{\rm eq}$, the Lorentz factor at which magnetic and electron energy densities are equal (assuming equality in eq. [25]). The very strong dependence of the electron energy density on Γ would lead to unacceptably high pressures in the jet if Γ were significantly smaller than $\Gamma_{\rm eq}$. Relativistic Lorentz factors (although not necessarily as large as $\Gamma_{\rm min}$) are also needed to avoid absorption of the 10 GeV photons on the synchrotron radiation produced in the jet. One may place an upper limit on Γ in terms of observational constraints on the central (nonblazar) UV luminosity. The only direct signatures of central UV sources in blazars are very weak UV excesses sometimes observed during the low-luminosity states of OVV quasars (Malkan & Moore 1986; Impey & Neugebauer 1988; Brown et al. 1989a). The luminosity $L_{\rm UV}$ of any such component in 3C 279 seems not to exceed 10^{46} ergs s^{-1} (Makino et al. 1989). Noting that $\tau L_{\rm UV}$ is likely to be at least a factor $\sim$10–100 smaller than $L_{\rm UV}$, and taking into account limits on the pattern propagation parameters (right-hand column of Table 1), we conclude that $\Gamma/\Gamma_{\rm min} \lesssim 2 f_p^{-1/3}$.

In addition to our constraints on bulk Lorentz factor, we derive plausible estimates for other properties of the jet and the ambient radiation field. We have already discussed the estimate for $\tau L_{\rm UV}$, which is consistent with only a percent or so of the central continuum being scattered or reprocessed. Both the magnetic and electron energy densities are consistent with typical values associated with jets at a fraction of a parsec from the nucleus, and with inferred pressures in the broad emission-line regions of AGNs. Finally, our estimates of γ–γ optical depths indicate that the observed gamma rays should be able to escape from the source (given plausible guesses for $f_{\rm XUV}^{\rm (diff)}$ and f_p).

Figure 1 presents a spectral decomposition of our model for 3C 279 with $E_{\rm ext} = 10$ eV, showing the separate contributions from beamed synchrotron radiation (S), SSC emission [C(S)], and Comptonized diffuse UV radiation [C(UV)]. In addition to representing the multifrequency data compiled by Hartman et al. (1992) (following Makino et al. 1989), we plot the Comptel data from Hermsen et al. (1993). We are able to fit all of the adopted observational constraints except for the X-ray flux, which we underpredict by a factor $\sim$10. This discrepancy could simply be the result of the X-ray and gamma-ray measurements having been made at different times. Note that a higher X-ray flux does not necessarily imply that the gamma-ray flux had to have been brighter at that time, since flares occurring at different radii (i.e., with different values of Δt) will generally exhibit different values of E_b (see § 5.4). Alternatively, the higher X-ray flux could result from the superposition of additional radiation sources, e.g., from the inner part of the jet. These would have lower break energies (§ 5.4), and therefore could dominate the X-ray flux without overproducing gamma rays.

Our model for 3C 279 predicts the value of $E_{C,\rm max}$, the maximum energy of the Comptonized component. The latter should exceed the maximum energy detected by EGRET by no more than a factor of a few; it is possible that the cutoff could be detected if EGRET manages to catch 3C 279 (with a long exposure) during another flaring episode. Note also that our estimate of the synchrotron self-absorption frequency, $\nu_{\rm syn,abs}$, fits very well with observational constraints. However, this agreement could be partly fortuitous since the low-frequency portion of the synchrotron spectrum probably includes emission from other regions in the jet. If so, the far-IR and submillimeter fluxes should not vary strongly during optical-UV flares, as seems to be the case in the data presented by Makino et al. (1989).

5.3. *Pattern Propagation Effects*

In Table 1 we show the full dependence of the model output parameters on the pattern propagation parameters (η, β_p', ϕ_p, and f_p), partly to illustrate that our model is relatively insensitive to the uncertain physical details expressed through these quantities. By far, the model is most sensitive to the bulk Lorentz factor of the fluid. The dependence of most quantities on the pattern propagation speed in the comoving frame, β_p', is particularly weak. Decreasing η, which corresponds to making each fluid element radiate during only a small fraction of the flare, increases the requirements on all comoving energy densities ($\propto \eta^{-1}$), on the γ–γ opacity to $\sim$10 GeV photons ($\propto \eta^{-1}$), and on the required luminosity in the diffuse ambient radiation field ($\propto \eta^{-4/3}$). For fixed $\Gamma/\Gamma_{\rm min}$ and $\eta \sim O(1)$, the quantities most affected by decreasing the pattern speed are, again, the energy densities (which increase $\propto f_p^{-1} \sim \Gamma^2/2\Gamma_p^2$). Note that $\tau_{\gamma\gamma}^{\rm (diff)}$ and $\tau L_{\rm UV}$, which depend on products of f_p and ϕ_p to

various powers, are not very sensitive to pattern speed in this limit, since the factors largely cancel one another.

5.4. *Scaling with* Δt

Why should significant dissipation of energy occur at a particular radius r (and with a particular variability timescale) rather than being distributed smoothly along the jet, as in Blandford's model? We suggest that the disturbances which eventually drive the dissipation are introduced near the base of the jet, where the bulk acceleration occurs. If this region in 3C 279 is located at a few Schwarzschild radii from a $\sim 10^8$ $M_\odot$ black hole, then the natural dynamical timescale Δt would be of order hours or days. Fluctuations in jet Lorentz factor of order $\Delta\Gamma \sim \Gamma$, separated by time Δt, would collide and dissipate only after traveling a distance $\sim \Gamma^2 c\,\Delta t$. Variability on longer timescales but with similar spectral properties might result from a train of shocks developing at this radius; according to this scenario we would not expect to see large-amplitude variability on much shorter timescales, even for wavelengths longward of the gamma rays. Alternatively, the central source could produce disturbances with a wide range of characteristic timescales. These would produce dissipation at various radii along the jet, with r scaling roughly as Δt (with Γ and Γ_p fixed). The scaling of flare properties with Δt is therefore an important diagnostic of our model.

To examine this scaling, we take $\Delta r \sim r$ and assume $\tau L_{\rm UV} \propto r^{-\mu}$, $B' \propto r^{-(1+\chi)}$, $E_{\rm ext} \propto r^{-\xi}$. The energy of the spectral break then scales according to

$$E_b \propto (\Delta t)^{2+2\mu-\xi}\,. \tag{26}$$

For reasonable values of μ and ξ (i.e., $\mu \geq 0$ and $\xi \sim 0$ for diffuse UV photons), E_b should increase with increasing variability timescale. The ratio of synchrotron flux to gamma-ray flux should scale as

$$\frac{\partial L_{\rm syn}/\partial \ln E}{\partial L_\gamma/\partial \ln E} \propto (\Delta t)^{\mu-2\chi}\,, \tag{27}$$

which could either increase, decrease, or remain constant with increasing Δt. The variation of $E_{C,\rm max}$ with Δt cannot be predicted without additional assumptions about the behavior of $\gamma_{\rm max}$, but we can predict that $\tau_{\gamma\gamma}^{(\rm diff)}(E_\gamma)$ should scale as $(\Delta t)^{-(1+\mu)}$, i.e. the γ–γ absorption depth should decrease with increasing variability timescale. Thus, very short timescale fluctuations in 3C 279, or fluctuations in sources more compact than 3C 279, might show a positive correlation between gamma-ray cutoff energy and flare timescale.

5.5. *Application to Mrk 421 and Other Blazars*

We have demonstrated explicitly that our one-zone model can explain most of the observed features in the continuum spectrum of 3C 279. Some of the other blazars observed by EGRET (Fichtel et al. 1993) show similar spectral features, including evidence for spectral steepening between the X-ray and gamma-ray bands, and we conjecture that these can be fitted by similar models. An obvious challenge to our model is whether it can explain the TeV gamma rays which have been observed from Mrk 421 (Punch et al. 1992). Our model for 3C 279 predicts a maximum photon energy of several tens of GeV, but much higher values of $E_{C,\rm max}$ would be expected in objects in which the synchrotron component extends to much higher energies than the $E_{\rm syn,max} \sim 5$ eV inferred for 3C 279. This is indeed the case for Mrk 421, in which the soft X-rays probably still belong to the synchrotron component (Makino et al. 1987). Observationally, there is a strong tendency for BL Lac objects (such as Mrk 421) to have synchrotron components extending up to X-ray energies, while the spectra of OVV quasars (e.g., 3C 279) steepen in the UV and show up harder in the X-ray band (Kii et al. 1992).

The greatest obstacle to modeling Mrk 421 with an external Comptonization model is the γ–γ pair production opacity due to the diffuse radiation field which surrounds the jet. This constraint can probably be overcome if the seed photons come from thermal IR emission by dust, rather than the UV photons assumed in our 3C 279 model. Differences in the principal source of seed photons may also be connected to the fact that Mrk 421 is a BL Lac object while 3C 279 is an OVV quasar. To date, very few BL Lac objects show evidence for thermal radiation by dust or a thermal UV excess, whereas the latter, in particular, is common in OVV quasars (Brown et al. 1989a, b). However, the presence of diffuse IR radiation in BL Lac cannot be ruled out. An additional advantage of producing the TeV radiation by Comptonizing IR photons is that the scattering takes place entirely in the Thomson regime ($\Gamma\gamma E_{\rm ext} < m_e c^2$), thus avoiding the depression in the spectrum associated with the Klein-Nishina regime. (This depression can be avoided for some model parameters; see Zdziarski & Krolik 1993.)

It is not known yet whether Mrk 421 and kindred objects exhibit a well-defined spectral break between the X-ray and gamma-ray bands. If they do not, then an SSC model may also provide a way to produce unbroken power-law spectra extending up to TeV energies. Such a model would necessarily involve scattering in the Klein-Nishina regime. As Zdziarski & Krolik (1993) showed, a *one-zone* SSC model for such objects *is not* viable unless the synchrotron luminosity is lower than the gamma-ray luminosity and the electron injection index (§ 4.1) $q = 2$. In the composite spectrum of Mrk 421 presented by Zdziarski & Krolik (1993), the former is not the case, but one must remember that the measurements of the X-ray (synchrotron) and gamma-ray (Compton) components were made several years apart.

We thank the referee, Alan Marscher, for his perceptive critique of the manuscript. This work has been supported in part by NSF grants AST 88-16140, AST 91-20599, and INT 90-17207, NASA grant NAG 5-2026 (*CGRO* Guest Investigator Program), and the Polish State Committee for Scientific Research grant 221129102.

REFERENCES

Begelman, M. C., & Sikora, M. 1987, ApJ, 322, 650
Bertsch, D. L., et al. 1993, ApJ, 405, L21
Blandford, R. D. 1993, in Compton Gamma-Ray Observatory, AIP Conf. Proc. 280, ed. M. Friedlander, N. Gehrels & D. J. Macomb (New York: AIP), 533
Blandford, R. D., & Königl, A. 1979, ApJ, 232, 34
Blandford, R. D., & Rees, M. J. 1978, in Pittsburgh Conf. on BL Lac Objects, ed. A. M. Wolfe (Pittsburgh: Univ. Pittsburgh Press), 328
Bloom, S. D., & Marscher, A. P. 1993, in Compton Gamma-Ray Observatory, AIP Conf. Proc. 280, ed. M. Friedlander, N. Gehrels & D. J. Macomb (New York: AIP), 578
Brown, L. M., et al. 1989a, ApJ, 340, 129
Brown, L. M., Robson, E. I., Gear, W. K., & Smith, M. G. 1989b, ApJ, 340, 150
Dermer, C. D. 1993, in Compton Gamma-Ray Observatory, AIP Conf. Proc. 280, ed. M. Friedlander, N. Gehrels & D. J. Macomb (New York: AIP), 541
Dermer, C. D., & Schlickeiser, R. 1993, ApJ, 416, 458

Dermer, C. D., Schlickeiser, R., & Mastichiadis, A. 1992, A&A, 256, L27
Fichtel, C. E., et al. 1993, in Compton Gamma-Ray Observatory, AIP Conf. Proc. 280, ed. M. Friedlander, N. Gehrels & D. J. Macomb (New York: AIP), 461
Ghisellini, G., & Maraschi, L. 1989, ApJ, 340, 181
Ginzburg, V. L., & Syrovatski, S. I. 1969, ARA&A, 7, 375
Hartman, R. C., et al. 1992, ApJ, 385, L1
Hermsen, W., et al. 1993, A&AS, 97, 97
Hunter, S. D., et al. 1993, ApJ, 409, 134
Impey, C. D., & Neugebauer, G. 1988, AJ, 95, 307
Jones, T. W., O'Dell, S. L., & Stein, W. A. 1974, ApJ, 188, 353
Kii, T., et al. 1992, in Frontiers of X-Ray Astronomy, ed. Y. Tanaka & K. Koyama (Tokyo: Universal Academy Press), 577
Königl, A. 1981, ApJ, 243, 700
Makino, F., et al. 1987, ApJ, 313, 662
Makino, F., et al. 1989, ApJ, 347, L9
Malkan, M. A., & Moore, R. L. 1986, ApJ, 300, 216
Maraschi, L., Ghisellini, G., & Celotti, A. 1992, ApJ, 397, L5
Marscher, A. P. 1993, in Space Telescope Sci. Inst. Symp. 6, Astrophysical Jets, ed. D. Burgarella, M. Livio, & C. O'Dea (Cambridge: Cambridge Univ. Press), in press
Marscher, A. P., & Gear, W. K. 1985, ApJ, 298, 114
Melia, F., & Königl, A. 1989, ApJ, 340, 162
Mushotzky, R. F., et al. 1978, ApJ, 226, L65
Punch, M., et al. 1992, Nature, 358, 477
Rees, M. J. 1967, MNRAS, 137, 429
Sikora, M., Begelman, M. C., & Rees, M. J. 1993, in Compton Gamma-Ray Observatory, AIP Conf. Proc. 280, ed. M. Friedlander, N. Gehrels & D. J. Macomb (New York: AIP), 598
Worrall, D. M., & Wilkes, B. J. 1990, ApJ, 360, 396
Zbyszewska, M. 1993, in Compton Gamma-Ray Observatory, AIP Conf. Proc. 280, ed. M. Friedlander, N. Gehrels & D. J. Macomb (New York: AIP), 608
Zdziarski, A. A., & Krolik, J. H. 1993, ApJ, 409, L33